CHROMSYMP. 2949

High-performance liquid chromatography of amino acids, peptides and proteins

CXXV[*]. Molecular dynamics simulation of *n*-butyl chains chemically bonded to silica-based reversed-phase high-performance liquid chromatography sorbents

Irene Yarovsky, Marie-Isabel Aguilar and Milton T.W. Hearn[*]

*Department of Biochemistry and Centre for Bioprocess Technology, Monash University, Wellington Road, Clayton,
Victoria 3168 (Australia)*

ABSTRACT

The molecular dynamics method has been applied to investigate the conformations of *n*-butyl ligands immobilised onto an amorphous silica surface analogous to those utilised with silica-based RP-HPLC sorbents. Three systems were constructed which corresponded to ligand densities of 1.64, 2.67 and 3.69 μmol/m^2. A number of parameters related to the structure of the sorbent materials were derived in order to characterise the molecular properties of each system. These parameters included the hydrocarbon layer thickness, the frequency of gauche conformations, the distance distribution for carbon atoms and the diffusion coefficients of individual atoms in the *n*-butyl ligands. From these properties, the positions of chains with respect to the surface as well as their mobility were estimated. It was found that at higher densities, the *n*-butyl chains are predominantly perpendicular to the surface while at low density they are highly tilted or lying almost parallel to the surface. The degree of ligand flexibility decreased with increasing surface density. Mobility of individual carbon atoms as well as chain disorder increased with distance from the surface for all ligand densities. The simulated properties of *n*-butyl chains immobilised to a silica surface correlated well with results obtained by Fourier transform IR and ^{13}C-cross polarisation magic angle spinning NMR experimental methods and statistical predictions of the behaviour of immobilised chains.

INTRODUCTION

High-performance liquid chromatography (HPLC) with microparticulate silica-based sorbents is now the central technique for the analysis and purification of many chemical and biological molecules. This popularity is due to a large number of factors, including the high reproducibility, selectivity and sensitivity of HPLC techniques. While significant advances continue to be made in chromatographic applications with high-performance adsorbents, there has been much less progress in the development of mechanistic models which describe, in detailed molecular terms, the interactive processes which occur between the immobilised stationary phase ligands, the mobile phase and the solute. This can be attributed, in part, to the lack of knowledge about the precise interactive structure and conformational properties of the immobilised ligands. The development of such knowledge would not only aid interpretation of re-

---

* Corresponding author.
[*] For Part CXXIV, see ref. 35.

76

I. Yarovsky et al. / J. Chromatogr. A 660 (1994) 75–84

tention mechanisms *per se* but also provide the basis for significant improvements in the design of new adsorbents.

Current understanding of the structure and relative dynamics of ligands immobilised to silica stationary phases has been largely derived from spectroscopic techniques [1–8]. For example, it has been demonstrated [1–6] by solid state NMR studies on *n*-alkylsilica reversed-phase sorbents that the mobility of the immobilised *n*-alkyl chains is dependent on the degree of functionalisation of the silanol groups, the composition of the *n*-alkyl groups, the extent of endcapping and the composition of the mobile phase. Fourier transform infrared (FT-IR) spectroscopy has also been used [9,10] with *n*-alkyl silicas to study the conformational disorder of immobilised *n*-alkyldimethyl ligands and has revealed a significant increase in the molecular ordering of the hydrocarbon ligands when immobilised compared to the corresponding non-immobilised but chemisorbed silanes. Additional information about the flexibility of *n*-alkyl ligands with silica-based stationary phases has also been indirectly obtained from chromatographic measurements. For example, the transitions which occur in the retention behaviour of solutes, when chromatographed on *n*-alkylsilicas under experimental conditions involving increases in temperature, have been related to the structural reordering of the ligand [11,12]. Furthermore, the extent of self assembly and association between two immobilised groups has been found to be dependent on the distance between their points of attachment [11]. Other studies have suggested that longer *n*-alkyl chains may exist as aggregates or clusters of chains under conditions of maximum ligand density [13]. In addition to revealing the effect of ligand density on ligand conformation, (which clearly affects chromatographic retention, resolution and peak shape), NMR studies have shown [3] that for dense ligand coverages, there is a steric masking of unreacted silanol groups present on the stationary phase surface.

Current theories of reversed-phase chromatography are based on very incomplete data on the distribution and conformation of the *n*-alkyl ligands bonded to the silica surface. A statistical theory has been developed to describe the mech-

anism of retention of small molecules in terms of partition or adsorption with *n*-alkyl ligands used in RP-HPLC [14–16]. The partition model involves the formation of a solute-sized cavity in the stationary phase which is followed by transfer of the solute from the aqueous cavity in the mobile phase to the stationary phase and closure of the cavity in the mobile phase. As a consequence, the partition model, in contrast to the adsorption model [17], predicts a critical role of the *n*-alkyl ligand density. These studies have also led to the prediction that the segments of the chain nearest to the silica surface are the most highly ordered and are thus aligned normal to the surface, and that increasing the surface density of the chains leads to increased ordering of the entire chain. As far as the effects of chain ordering on solute retention is concerned, there are two principal predictions by this statistical theory. Firstly, it is anticipated from entropic considerations that a solute will prefer to interact with the ends of the chain rather than with the immobilised section of the chain. Secondly, as the surface density approaches its maximum value, the solute is predicted to become increasingly expelled from the stationary phase due to the entropic effects of chain ordering. At low ligand densities, solute partitioning should increase linearly with the surface coverage of the ligand chains. The partition coefficient should reach a maximum at the point at which neighbouring interactions between chains become significant and at a maximum surface density, no solute will partition into the stationary phase. Although this partitioning dependence on chain density is not directly observable in chromatographic retention, experimental data of Sentell and Dorsey [18] support these theoretical predictions. A major conclusion from these experiments is that the chain organisation of the stationary phase plays a major role in the retention. These results can be contrasted with predictions of the solvophobic or adsorption theory [17] which does not incorporate the entropic role of the stationary phase ligand structure. The evolution of a comprehensive mechanistic description of the chromatographic process at the molecular level requires significantly more detailed information on the microscopic characteristics of the *n*-alkyl ligand struc-

ture in terms of the molecular dynamics of individual backbone atoms as they interact with the surrounding solvent or the specific solutes. Advances in molecular modelling techniques provide a powerful approach to study the conformational properties of *n*-alkyl chain molecules in solution [19–22] as well as immobilised onto surfaces [23–29]. Availability of sophisticated computer graphics systems which allow the construction of complex molecular models, together with advanced forcefields for the calculation of potential energy surfaces, has made it possible to create and investigate the models of chromatographic support materials.

The aim of this work involved simulation of the reversed-phase chromatographic environment for further modelling of the retention process for various biological molecules. In the present study, a molecular dynamics method has been applied to the study of the conformational and dynamical properties of *n*-butyl ligands immobilised onto silica.

MATERIALS AND METHODS

Molecular model

n-Butyldimethyl ligands were covalently bonded to a model amorphous silica surface [23,24] with three different surface densities. The structure of a single attached ligand is shown in Fig. 1. The silica lattice contained 285 silicon and 570 oxygen atoms with the total hydroxyl groups surface density equal to 6.57 μmol/m^2. Atomic coordinates for the silica matrix determined previously [23,24] were fixed during the simulation.
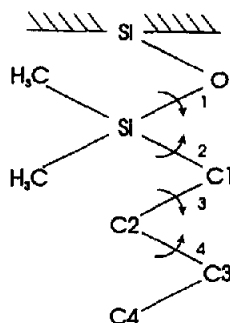
Three molecular systems were designated A,

Fig. 1. Schematic structure of an *n*-butyldimethylsilyl ligand attached to a silica surface indicating the torsion angles.

B and C, corresponding to the surface ligand density 3.69, 2.67 and 1.64 μmol/m^2, respectively. Periodic boundary conditions with unit cell dimensions [28.5 × 28.5 × 25.0 Å] were applied to mimic an infinite *n*-alkyl modified chromatographic surface. The initial conformation of the chains was all-*trans* and the chains were oriented normal to the surface. Table I summarises the main parameters of the simulated systems. Computational results were obtained using software programs from Biosym Technologies (San Diego, CA, USA): dynamics calculations were performed with *Discover* and graphic displays were created using *InsightII*. All calculations were performed on a CONVEX C210 supercomputer.

Computational method

The molecular dynamics (MD) simulation method was applied to the molecular systems described above. The potential energy of the system was calculated as a sum of the terms reflecting energy needed to stretch bonds, bend

TABLE I

MOLECULAR DETAILS OF SIMULATED SYSTEMS

System name	Ligand surface density (μmol/m^2)	Hydroxyl surface density (μmol/m^2)	Surface area per ligand (Å^2)	Near neighbour spacing (Å)	Number of atoms	Hydrocarbon layer thickness (Å)
A	3.69	2.88	45.12	6.71	1420	5.63
B	2.67	3.90	62.48	7.90	1315	5.45
C	1.64	4.93	101.53	10.08	1210	3.43

bond angles, rotate torsion angles as well as the terms representing the non-bond Van der Waals and electrostatic interactions. The Consistent Valence Forcefield [30] from the Biosym Library, which is parameterised for the silicon atom, was used to approximate the potential energy of the simulated systems. The non-bonded interactions for pairs of atoms separated by distances greater than a cutoff value of 12 Å were neglected. The neighbour list was updated every 20 steps. A distance-dependent dielectric constant was used to model the effect of solvent. Although such a model cannot account for the structural contribution of solvent, it still provides a screening effect of solvent on electrostatic interactions [30, and references therein]. The aim of this study was to create a molecular model of a reversed-phase sorbent which is physically consistent with available experimental data on ligand structure which are obtained in various solvent environments (including dry). As the end point of these investigations is the molecular modelling of the peptide–sorbent–solvent interactions, it was considered appropriate at the initial stage to use the approximation of a distance-dependent dielectric constant rather than the use of explicit solvent which would significantly increase the computational time of the experiments.

To avoid bad contacts arising from the initial model building, the energy of each system was first minimised by steepest descents followed by conjugate gradients method until the derivatives decreased to 1 kcal mol^{-1} Å^{-1}. Systems were then subjected to the constant volume molecular dynamics with periodic boundary conditions. Temperature of simulation was set to 300 K. Initial velocities were randomly assigned according to a Maxwell–Boltzmann distribution for the given temperature. The equations of motion were solved using the Verlet algorithm [31] with the integration time step of 1 fs. The initial equilibration stage, in which the temperature was adjusted by scaling the velocities, was continued until such properties as total energy, temperature, and *trans* fraction of chain torsion angles had stabilised. The duration of equilibration runs was 20–40 ps (20 000–40 000 time steps) depending on the size of the system. An equilibration period was followed by a data collection stage of 100 ps (100 000 time steps) in which Berendsen's method of a weak coupling of the system to a temperature bath at 300 K was applied [32]. The atomic coordinates were stored on disk every 100 time steps for analysis.

RESULTS AND DISCUSSION

Hydrocarbon layer thickness and surface accessibility

The aim of this study was to create a molecular model of an RP-HPLC system to allow the simulation of the reversed-phase chromatographic process. Following molecular dynamics, a number of physical parameters were derived to characterise the molecular properties of each system. The thickness of the hydrocarbon layer is an important quantity which can be used for the estimation of the position of the ligands with respect to the surface as well as accessibility of the unreacted surface silanols to solvent and solute under chromatographic conditions. To assess the average thickness of the hydrocarbon layer in the systems under investigation, the average distances between the terminal methyl group (C4 atom) and the mean Si-plane were calculated. The mean Si-plane was constructed as an average plane containing Si atoms from the upper layer of the surface of the molecular models displayed in Figs. 2–4. The Si–O–Si(CH$_3$)$_2$– atoms (Fig. 1) were considered as part of the chains thus contributing to the thickness value.

It was found that the average thickness of the most dense hydrocarbon layer (system A) amounts to 5.63 Å (Table I). For the intermediate density (system B) it is equal to 5.45 Å while for the lowest density (system C), the thickness is equal to 3.43 Å. The value for the more dense systems (A, B) is similar to the thickness of the starting structure which was about 6 Å and corresponds to fully extended (*i.e.* all-*trans*) chain conformation (the value of the thickness of the extended configuration is an estimate as any relaxation of the starting structure which was built up manually results in changes in the chain conformation). The small decrease in the thickness of systems A and B
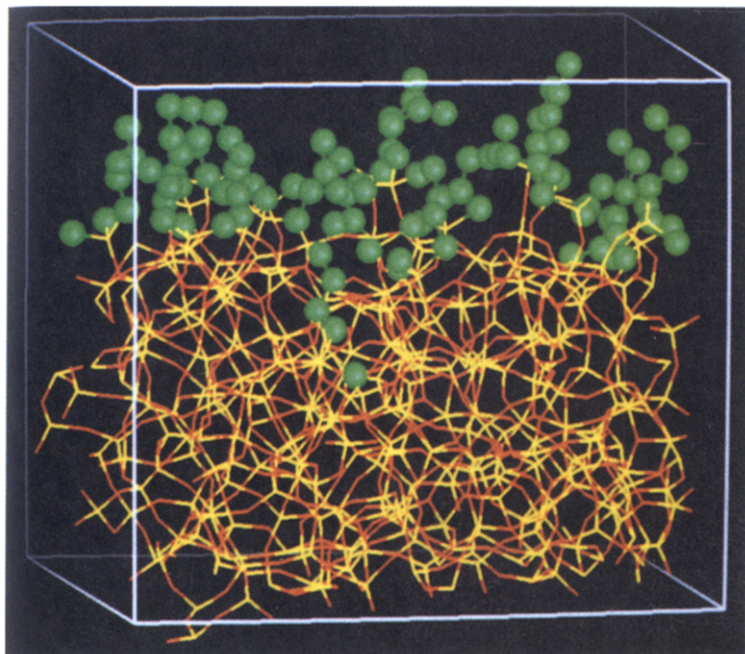
Fig. 2. Instantaneous conformation of n-butyl ligands immobilised onto amorphous silica with ligand density = 3.69 μmol/m^2, taken from the later stages of the dynamics run. Atoms are colour-coded as follows: silicon, yellow; oxygen, red; carbon, green. Carbon atoms are presented in a space filling mode. Hydrogens are not displayed.
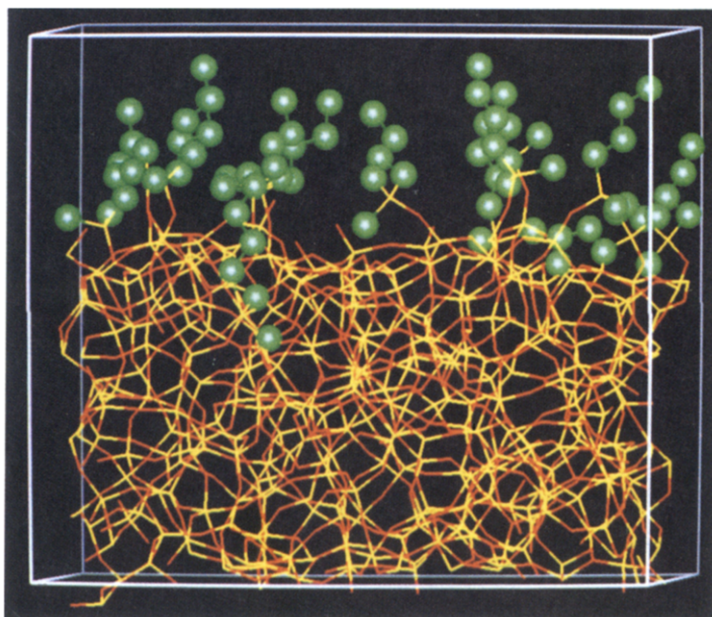

Fig. 3. Instantaneous conformation of n-butyl ligands immobilised onto amorphous silica with ligand density = 2.67 μmol/m^2, taken from the later stages of the dynamics run. See Fig. 2 for colour codes.
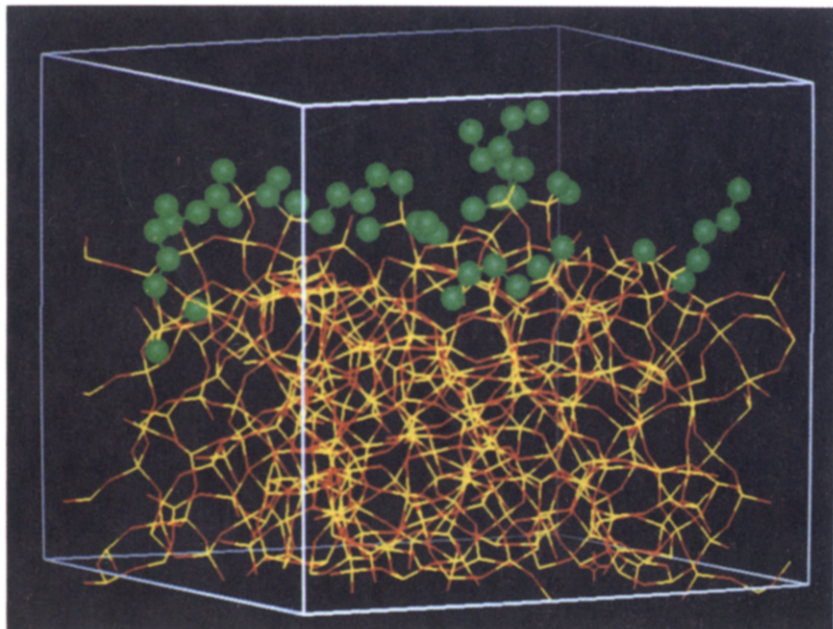
Fig. 4. Instantaneous conformation of *n*-butyl ligands immobilised onto amorphous silica with ligand density = 1.64 μmol/m^2, taken from the later stages of the dynamics run. See Fig. 2 for colour codes.

indicates that the equilibrium positions of the chains are normal to the surface or slightly tilted (Figs. 2 and 3) which is a consequence of the steric restrictions imposed on each chain by the neighbouring ligands. These results also show that the *trans* conformation is predominant for higher ligand densities. For the lowest ligand density system C, the hydrocarbon layer thickness is much lower which demonstrates that the *n*-alkyl chains are bent, highly tilted or are lying almost parallel to the surface (Fig. 4). The near neighbour spacing (Table I) for system C is 2.18 Å larger than for system B, while there is a much smaller difference between systems A and B, *i.e.* 1.19 Å. Thus for the lowest ligand density system, the *n*-alkyl chains possess much more space for movement which results in their ability to cover the surface.

The average thickness of the hydrocarbon layer can also be used to estimate the solute approach distance taking into account allowed van der Waals interaction distances. Thus in the higher ligand density systems a solute molecule cannot approach the surface closer than about 6–7 Å (because of the high ligand density and thick hydrocarbon layer) while for the lowest

density the solute can approach the surface to 4–5 Å which could significantly increase the solute interaction with any unreacted silanols and influence the retention. At the same time it should be noticed that the ability of chains at low density to form a bent structure and to cover the surface may create an additional protection for unreacted silanols.

In addition, the total solvent-accessible surface area of each system was calculated using the Connolly algorithm [33] with a water probe radius of 1.4 Å. The accessible area with chains in the starting conformations (*i.e.* all-*trans* and perpendicular to the silica surface) was compared with the average surface accessibility of equilibrium conformations stored during the dynamics run. The percentage decrease in surface accessibility was 11.20, 6.63 and 1.38% for systems A, B and C, respectively, indicating that the percentage decrease in surface accessibility was highest for the high density system A. This result demonstrates that for *n*-butyl ligands, the surface silanols are more highly protected with higher ligand densities. In spite of the ability of the low density ligands to approach very close to the silica surface, this extra surface protection is still

low compared to the higher ligand density systems.

Trans–gauche statistics

The codes used for assignment of the hydrocarbon chain dihedral angles were the customary g^+, t, and g^-, corresponding to the three intervals: (0° to 120°), (120° to −120°), and (−120° to 0°) respectively. The state of the internal dihedral angles of a molecule (g^+, t, g^-) is the factor determining the overall orientation of the molecule with respect to the surface. The overall proportion of *gauche* conformation in the chains is 14, 15, and 25% for the systems A, B and C, correspondingly. This result reflects the fact that the number of *gauche* defects increases as the spacing between the ligands increases which is also in agreement with the theoretical predictions [16].

The fractions of the *gauche* conformation for each dihedral angle along the C4 chain are shown in Fig. 5 for the different ligand densities. The numbers of torsion angles are assigned as shown in Fig. 1. Torsion angles 1 and 2 describe the geometry of ligand attachment to the silica surface. It can be seen from Fig. 5 that a relatively high proportion of *gauche* conformation for torsion 1 is established for all systems. This results in the perpendicular orientation of
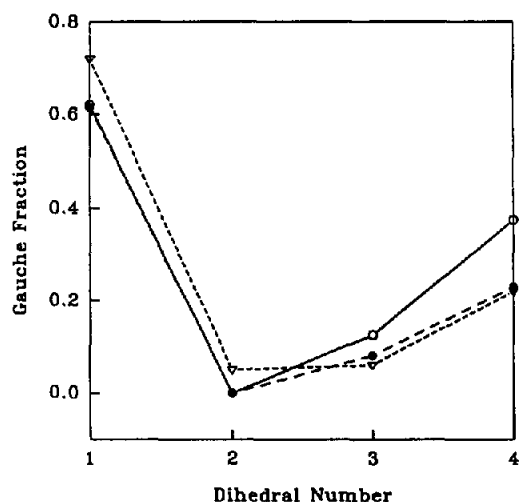

Fig. 5. Fraction of gauche dihedral angles in *n*-butyl ligands as a function of dihedral number. $O = 1.64$ μmol/m^2; $\bullet$ = 2.67 μmol/m^2; $\nabla = 3.69$ μmol/m^2.

the O–Si bond to the surface. The frequency of *gauche* conformations at this position increases with ligand density. This result indicates that the probability of chain orientation which is perpendicular to the surface at this position is higher for high density systems which would be anticipated from steric considerations. Torsion number 2 is predominantly in a *trans* conformation, thus maintaining the chain orientation to the surface created by the conformation of torsion number 1.

The relative statistics of the next two torsion angles number 3 and 4 is determined by an energetically inexpensive internal rotation about single C–C bonds. Theoretically, the structure with a higher chain density will prefer a *trans* conformation which sterically allows more dense packings. This steric effect is reflected by an increase in the *gauche* population for dihedral angle 4 for the low density system. In terms of the overall *n*-alkyl chain geometry, most of the *gauche* conformations are concentrated around the C2–C3 bond demonstrating that the end-*gauche* defect is the most probable for the *n*-butyl ligands and that the degree of order of the carbon chains increases near the silica surface. This observation is also in agreement with Fourier transform infrared spectroscopy studies of RP-HPLC ligands [9] and is consistent with the theoretical treatment of Dorsey and Dill [16].

End-to-end distance distribution functions

To characterise the average length of the hydrocarbon chains, the distribution function of the end-to-end distance, *i.e.* the distance between C1 and C4 atoms of the ligands, was constructed and is shown in Fig. 6. It can be seen that there are 2 peaks which correspond to distances of 3.25 Å and 3.95 Å between C1 and C4. The first peak of the distribution function ($r = 3.25$ Å) corresponds to the *gauche* conformation for the C1–C2–C3–C4 torsion angle. It can be seen in Fig. 6 that the probability of the *gauche* conformation is highest for the low density system C. In contrast, the probability of the end-to-end distance of 3.95 Å which corresponds to the all-*trans* conformation is higher for systems A and B.
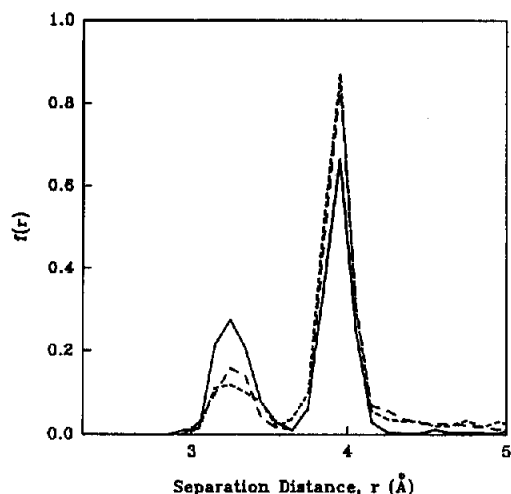
Fig. 6. End-to-end distance distribution of n-butyl ligands at different densities. ——— = 1.64 μmol/m^2; – – – – = 2.67 μmol/m^2; ---- = 3.69 μmol/m^2.

Fig. 7. Mean squared displacements (MSD) of carbon atoms in n-butyl ligands as a function of time for ligand density = 2.67 μmol/m^2.

Mobility

Differences in the mobility of the n-butyl ligands can also be revealed by studying the dynamic behaviour of the carbon atoms. The time dependence of the average mean squared displacements (MSD) of individual carbon atoms over the all chains in the simulation and multiple time origins t_0 were calculated according to the following relationship:

$$MSD = [\Delta R(t)]^2 = \sum \langle |r_i(t + t_0) - r_i(t_0)|^2 \rangle \quad (1)$$

where R is the average distance travelled and r_i represents the coordinates of atom i. Fig. 7 shows the dependence of the MSD over time for the individual carbon atoms in System B. The overall appearance of these plots is similar for all the systems under investigation. To estimate the relative mobilities of individual carbon atoms diffusion coefficients (D) for these atoms were calculated. Diffusion constants were obtained using the Einstein relation [34] as follows:

$$2tD = 1/3 \lim_{t \to \infty} \langle [\Delta R(t)]^2 \rangle \quad (2)$$

A plot of the calculated diffusion constants for individual carbon atoms in different systems is given in Fig. 8. It can be seen from Fig. 7 and Fig. 8 that for all ligand densities, the mobility
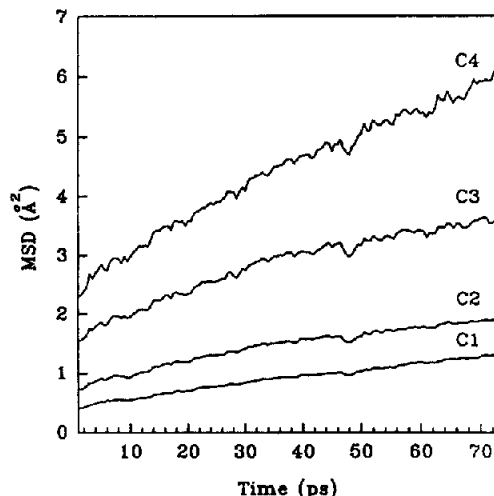
increases from the C1 atom to the C4 atom, *i.e.* atoms closer to the surface are more restricted by immobilisation than the remote atoms. This result is in agreement with ^{13}C cross polarization magic angle spinning NMR spectroscopy measurements of the proton relaxation times in the rotating coordinate system which have been
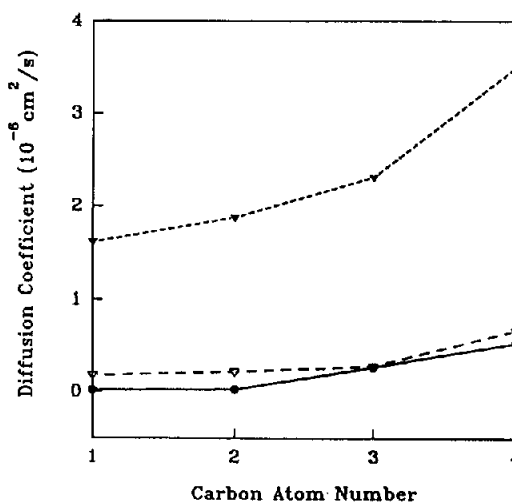

Fig. 8. Diffusion coefficients of individual carbon atoms of n-butyl ligands at different ligand densities. ▼ = 1.64 μmol/m^2; ▽ = 2.67 μmol/m^2; ● = 3.69 μmol/m^2.

described as a measure of mobility of the alkyl chains [2]. It is interesting to notice that the increased mobility of the atoms remote from the surface also correlates with the increased number of *gauche* defects around the C1–C2–C3–C4 dihedral angle (Fig. 5).

The results obtained for the mobility of *n*-butyl ligands are also consistent with the results of previous NMR studies [2] in which a ligand density of 3.5 ± 0.2 μmol/m^2 was employed which corresponds to our highest density system A. These workers found that the overall mobility of *n*-butyl ligands was relatively low, indicating a low motional freedom for all the carbon atoms of this phase, and increases slightly for the terminal methyl group which is in agreement with our simulation (Fig. 7).

It is evident from Fig. 8 that the mobility of carbon atoms is highest in the lowest density system C. This observation also can be explained by steric restrictions resulting from the different near neighbour ligand spacing at different densities. The mobility of ligands in systems A and B is very low and increases dramatically in the lowest density system C where chains possess much more space for movement which results in a higher diffusion coefficient for individual carbon atoms. This result also correlates with the general conclusion of previous NMR studies [4] which showed that *n*-alkyl chain mobility is a function of surface coverage, since the available space of a single chain decreases with increasing coverage.

CONCLUSIONS

In the present study, a molecular model of an *n*-butylsilica sorbent has been constructed. The molecular properties of the model have been characterised by a number of physical parameters. The results of the conformational analysis indicate that the simulation reproduces the behaviour of the *n*-alkyl ligands which is qualitatively consistent with published spectroscopic data. These studies are currently being extended to the simulation of *n*-octyl and *n*-octadecyl sorbents, with the model presented here used to further study the molecular basis of the chromatographic process in RP-HPLC.

REFERENCES

1 K.D. Lork, K.K. Unger, H. Bruckner and M.T.W. Hearn, *J. Chromatogr.*, 476 (1989) 135.
2 B. Pfleiderer, K. Albert, K.D. Lork, K.K. Unger, H. Bruckner and E. Bayer, *Angew. Chem., Int. Ed. Engl.*, 28 (1989) 327.
3 B. Buszewski, Z. Suprynowicz, P. Staszczuk, K. Albert, B. Pfleiderer and E. Bayer, *J. Chromatogr.*, 499 (1990) 305.
4 E. Bayer, A. Paulus, B. Peters, G. Laupp, J. Reiners and K. Albert, *J. Chromatogr.*, 364 (1986) 25.
5 G. Lindgren, B. Lundstrom, I. Kallman and K.-A. Hansson, *J. Chromatogr.*, 296 (1984) 83.
6 H.A. Claessens, J.W. De Haan, L.J.M. Van de Ven, P.C. De Bruyn and C.A. Cramers, *J. Chromatogr.*, 436 (1988) 345.
7 P.B. Wright, E. Lamb, J.G. Dorsey and R.G. Kooser, *Anal. Chem.*, 64 (1992) 785.
8 M.E. Montgomery Jr., M.A. Green and M.J. Wirth, *Anal. Chem.*, 64 (1992) 1170.
9 L.C. Sander, J.B. Callis and L.R. Field, *Anal. Chem.*, 55 (1983) 1068.
10 D.E. Leyden, D.S. Kendall, L.W. Burggraf, F.J. Pern and M. DeBello, *Anal. Chem.*, 54 (1982) 101.
11 S.S. Yang and R.K. Gilpin, *J. Chromatogr.*, 449 (1988) 115.
12 D. Morel, K. Tabar, J. Serpinet, P. Claudy and J.M. Letoffe, *J. Chromatogr.*, 395 (1987) 73.
13 C.H. Lochmuller, A.S. Colbarn, M.L. Hunnicutt and J.M. Harris, *Anal. Chem.*, 55 (1983) 1344.
14 K.A. Dill and P.J. Flory, *Proc. Natl. Acad. Sci. USA*, 77 (1980) 3115.
15 K.A. Dill, *J. Phys. Chem.*, 91 (1987) 1980.
16 J.G. Dorsey and K.A. Dill, *Chem. Rev.*, 89 (1989) 331.
17 Cs. Horváth, W. Melander and I. Molnar, *J. Chromatogr.*, 125 (1976) 125.
18 K.B. Sentell and J.G. Dorsey, *Anal. Chem.*, 61 (1989) 930.
19 E. Egberts and H.J.C. Berendsen, *J. Chem. Phys.*, 89 (1988) 3718.
20 J.P. Ryckaert, I.R. McDonald and M.L. Klein, *Mol. Phys.*, 67 (1989) 957.
21 I.L. Shamovsky and I.Yu. Yarovskaya, *J. Molec. Struct. (Theochem.)*, 236 (1991) 333.
22 S. Karaborny and S. Toxvaerd, *J. Chem. Phys.*, 97 (1992) 5876.

84

I. Yarovsky et al. / J. Chromatogr. A 660 (1994) 75–84

23 S.M. Levine and S.H. Garofalini, *Surf. Sci.*, 163 (1985) 59.

24 S.M. Levine and S.H. Garofalini, in F.L. Galeener, D.L. Griscom and M.J. Weber (Editors), *Defects in Glasses, Proc. Material Research Society Symposia, Boston, MA, December 2–4, 1985*, Vol. 61, Materials Research Society Press, 1986, p. 29–37.

25 J. Hautman and M.L. Klein, *J. Chem. Phys.*, 91 (1989) 4994.

26 J. Hautman and M.L. Klein, *J. Chem. Phys.*, 93 (1990) 7483.

27 A. Biswas and B.L. Schurmann, *J. Chem. Phys.*, 95 (1991) 5377.

28 N.G. Almazza, E. Enciso and F.J. Bermejo, *J. Chem. Phys.*, 96 (1992) 4625.

29 T.K. Xia, J. Ouyang, M.W. Ribarsky and U. Landman, *Phys. Rev. Lett.*, 69 (1992) 1967.

30 *Discover User Guide*, Version 2.9.0., Biosym Technology, San Diego, CA, 1993.

31 L. Verlet, *Phys. Rev.*, 159 (1967) 98.

32 H.J.C. Berendsen, J.P.M. Postma, W.F. van Gunsteren, A. DiNola and J.R. Haak, *J. Chem. Phys.*, 81 (1984) 3684.

33 M.L. Connolly, *Science*, 221 (1983) 709.

34 M.P. Allen and D.J. Tildesley, *Computer Simulation of Liquids*, Clarendon Press, Oxford Science Publications, Oxford, 1987.

35 G. Dasari, I. Prince and M.T.W. Hearn, *J. Chromatogr.*, 631 (1993) 115.